Local and cooperative structural transitions of double-stranded DNA in choline-based deep eutectic solvents

Fatemeh Fadaei, Mariagrazia Tortora, Alessandro Gessini, Claudio Masciovecchio, Jacopo Vigna, Ines Mancini, Andrea Mele, Jan Vacek, Babak Minofar, Barbara Rossi

PII: S0141-8130(23)05342-4

DOI: https://doi.org/10.1016/j.ijbiomac.2023.128443

Reference: BIOMAC 128443

To appear in: *International Journal of Biological Macromolecules*

Received date: 25 August 2023

Revised date: 20 November 2023

Accepted date: 22 November 2023

Please cite this article as: F. Fadaei, M. Tortora, A. Gessini, et al., Local and cooperative structural transitions of double-stranded DNA in choline-based deep eutectic solvents, *International Journal of Biological Macromolecules* (2023), https://doi.org/10.1016/j.ijbiomac.2023.128443

Local and cooperative structural transitions of double-stranded DNA in choline-based deep eutectic solvents

Fatemeh Fadaei[1], Mariagrazia Tortora[2,3], Alessandro Gessini[3], Claudio Masciovecchio[3], Jacopo Vigna[4], Ines Mancini[4], Andrea Mele[5], Jan Vacek[6], Babak Minofar[1*] and Barbara Rossi[3,4*]

1. *Faculty of Science, University of South Bohemia in České Budějovice, Branišovská 1645/31A, 37005 České Budějovice, Czech Republic*
2. *AREA SCIENCE PARK, Padriciano, 99, 34149 Trieste, Italy*
3. *Elettra-Sincrotrone Trieste, S.S. 114 km 163.5, Basovizza, 34149, Trieste, Italy*
4. *Laboratory of Bioorganic Chemistry, Department of Physics, University of Trento, Via Sommarive, 14 - 38123 Povo Trento, Italy*
5. *Department of Chemistry, Materials and Chemical Engineering ''G. Natta'', Politecnico di Milano Piazza L. da Vinci 32, 20133, Milano, Italy*
6. *Department of Medical Chemistry and Biochemistry, Faculty of Medicine and Dentistry, Palacky University, Hnevotinska 3, 775 15 Olomouc, Czech Republic*

* barbara.rossi@elettra.eu, babakminoofar@gmail.com

ABSTRACT (max 200 words)

The possibility of using deep eutectic solvents (DESs) as co-solvents for stabilizing and preserving the native structure of DNA provides an attractive opportunity in the field of DNA biotechnology. The rationale of this work is a systematic investigation of the effect of hydrated choline-based DES on the structural stability of a 30-base-pair double-stranded DNA model *via* a combination of spectroscopic experiments and MD simulations. UV absorption and CD experiments provide evidence of a significant contribution of DESs to the stabilization of the double-stranded canonical (B-form) DNA structure. Multi-wavelength synchrotron UV Resonance Raman (UVRR) measurements indicate that the hydration shell of adenine-thymine pairs is strongly perturbed in the presence of DESs and that the preferential interaction between H-bond sites of guanine residues and DESs is significantly involved in the stabilization of the dsDNA. Finally, MD calculations show that the minor groove of DNA is significantly selective for the choline part of the investigated DESs compared to the major groove. This finding is likely to have a significant impact not only in terms of thermal stability but also in the modulation of ligand-DNA interactions.

Keywords: deep eutectic solvents, nucleic acids, synchrotron UV resonance Raman, circular dichroism, molecular dynamics simulation

1. INTRODUCTION

The solvent for the dissolution and storage of bio-macromolecules is a key factor in preventing their degradation and other adverse effects on their functionality. Specifically, the long-term stability of nucleic acids in aqueous media can be affected, *inter alia*, by temperature, pH, and ionic strength, leading to denaturation of the functional helix structure [1,2]. Common strategies used for the preservation of nucleic acid integrity include the storage of specimens below 0 °C, freeze-drying methods, or the use of reagents that deactivate nuclease. However, these storage and preservative approaches require the use of additives that can be cytotoxic or carcinogenic. The reliance on DNA in an aqueous medium as a conventional solvent is also one of the most critical bottlenecks in DNA technology and the development of new DNA-based devices.

The addition of salts and/or organic co-solvents may be a possible strategy to enhance the conformational stability of nucleic acids in aqueous solution [3-6]. These molecules can directly bind

with DNA in place of water but the presence of a suitable concentration of so-solvents can also induce changes in the DNA hydration shell through the destruction of the H-bonds structure of water, thus affecting the stability of DNA. It has been demonstrated that aqueous solutions containing up to a few tens of wt/% of organic co-solvents do not significantly affect the DNA base pairing but tend to disrupt the weaker interactions of flexible residues [5]. However, higher concentrations (>40 %) of formamide, methanol, DMSO and diethylsulfoxide in water lead to a destabilization of double-stranded DNA, due to the establishment of H-bonds and hydrophobic interactions of these co-solutes with the nucleotide bases [6-8]. Some experimental studies revealed that the thermal stability of DNA is remarkably enhanced by the presence of glycerol in water [3] and that the duplex structure of nucleic acids is maintained even in an aqueous solution of 99 % glycerol [6]. This effect has been mainly ascribed to the solvophobic interactions of glycerol with DNA which seem to be the dominant factor in maintaining the structure of nucleic acids [6]. The thermal stability of DNA in water/dioxane and water/ethylene glycol solutions has been investigated as a function of the different compositions of the mixtures [4]. The experimental results suggest that, at a relatively low content of co-solvents, the melting temperature of the DNA duplex is mainly determined by the screening of charges due to the electrical permittivity of the solution.

For the past two decades, ionic liquids (ILs), both neat and hydrated, have received attention as valid alternatives to traditional solvents for DNA processing and preservation [9]. Although the impact of these compounds on the properties of DNA strongly depends on their composition, the general behaviour of IL towards nucleic acid duplexes is determined by specific interactions of the IL components with DNA grooves [9,10].

Deep eutectic solvents (DESs), first introduced by Abbot and co-workers [11], share many benign properties with ILs such as low (or negligible) vapour pressure, thermostability, and tunability of the chemical-physical properties, with the benefit of better degradability and lower toxicity than ILs [12]. Besides this, DESs are generally easy to prepare by simply mixing their constituents, which in turn can be chosen to be biodegradable and renewable. These properties have turned DESs into a rapidly emerging class of 'green' solvents or co-solvents for many biological applications, including the storage and manipulation of nucleic acids [13-20]. Indeed, the first and archetypal DES mixture, choline chloride-urea in a 1:2 molar ratio (often referred to as *reline*), was successfully used in both pure liquid form or in aqueous solution as a medium for G-quadruplex DNA sequences, which exhibited higher structural stability than in the usual water solutions [16,17,19]. Molecular dynamics (MD) simulations suggested that the hydrogen bonds (H-bonds) formed between reline and G-quadruplex DNA are responsible for the persistence of the tetradic structures observed even at high temperatures [17]. The stability of DNA secondary structures in anhydrous choline chloride/urea DES was first explored by Mamajanov *et al.* [21] on a 32-base-pair DNA sequence. Circular dichroism experiments revealed that DNA can form a stable duplex in neat reline at room temperature, indicating reline to be a suitable alternative solvent for long-term nucleic acid storage [21,22]. This effect has been attributed to the specific interactions between choline chloride (ChCl)-based DES and DNA, with the establishment of long-lasting binding interactions of choline ions with DNA [23]. Since choline ions have a high affinity for A-T base pairs, the multiple hydrogen bonds formed between choline and the DNA structure seem to be responsible for the preservation of the conformation of A-T-rich DNA duplexes dissolved in a choline-based DES [21,23]. Experimental evidence of the high solubility and long-term chemical integrity of DNA dissolved in other biocompatible choline chloride-based DESs has also been reported [24]. However, some of these studies provided evidence

that the melting transition midpoint of DNA is lower in pure choline-based DES than in the aqueous solutions, suggesting a depletion of the duplex stability under fully dehydrated conditions at high temperatures [21,22]. This effect has been attributed both to the distinct solvent properties of the choline-based DES towards DNA and the elimination of bulk water [21]. On the other hand, it has been observed that the double helical structure of the DNA is maintained even in hydrated tetrabutylammonium bromide-based DES up to a concentration of 25% of DES in water [25]. In summary, these results suggest that the use of DES/water mixtures as alternative solvents for DNA can effectively stabilize nucleic acid structures thanks to the unique combination of interactions between water, DES, and the biomolecule [13]. Indeed, the controlled addition of water can drastically change the supramolecular organization of DESs and their properties, thus representing an efficient way to tune their solvation behaviour for specific applications [13,26].

In this work, we aim to explore the thermal stability of a 30-base pair double-stranded DNA structure in aqueous solutions of three different choline-based DESs. Our molecular approach, based on circular dichroism (CD), UV absorption, and synchrotron radiation-UV Resonance Raman spectroscopy (SR-UVRR) experiments together with molecular dynamics (MD) simulations, enables us to probe base stacking, hydrogen bonding, and electrostatic interactions that contribute to the complex melting pathway of DNA. The effects of hydrated DESs on the local and cooperative structural transitions of DNA during its thermal denaturation were detected and discussed in the light of i) the combination of different HBD and HBA components of DES and ii) the competition between water and DES in the spine of hydration of the DNA structure. The combined experimental and simulation analyses provide a deeper understanding, at a molecular level, of the thermal stability and conformational properties of nucleic acids in the presence of hydrated choline-based DESs that could be crucial for developing a new generation of unconventional solvents for biomolecules.

2. MATERIALS AND METHODS

2.1. Chemicals and sample preparation

Fully complementary oligonucleotides (sequence of strand 1: AAC CCA GAT GTC CTA CAG GAT AGC TCG CAG; 53% of GC pairs, without 5-phosphate termination, 9184.94 Da) were synthesized by VBC Genomics (Vienna, Austria). The double-strand DNA (dsDNA) was prepared at a 100 μM duplex concentration in Tris buffer 10 mM at pH 7.4 by mixing the single strands in the same molar ratio, heating for 5 minutes at 90 °C and slowly cooling down to room temperature.

Choline chloride (ChCl), glycerol (Gly) and urea (U) were purchased from Sigma Aldrich, whereas choline acetate (ChOAc) was from Iolitec. They were dried under vacuum with phosphorus pentoxide for 48 h to avoid water contamination before use. ChCl:U, ChCl:Gly and ChOAc:U DESs (see chemical structures reported in Fig. S1) were prepared by mixing the components in a molar ratio of 1:2, respectively, and heating at ~80 °C with stirring until homogeneous and viscous liquids were formed. For the samples of dsDNA dissolved in hydrated DES, each DES was added to a solution of dsDNA at 100 μM and diluted with 10 mM Tris buffer at pH 7.4 to reach a final concentration of 150 mM of DES and 10 μM of dsDNA, corresponding to a molar ratio of DES:base pair (bp) of 500:1. For dsDNA dissolved in hydrated ChCl:U, three further concentrations of 53 mM, 80 mM, and 120 mM were analyzed, corresponding to a ratio DES:bp of 177:1, 267:1 and 400:1, respectively. All the solutions were freshly prepared before measurements and appeared transparent before and after the thermal heating.

2.2. SR-UVRR measurements and data analysis

Multi-wavelength UV resonance Raman spectra were collected by using the synchrotron-based UVRR set-up available at the BL10.2-IUVS beamline of Elettra Sincrotrone Trieste (Italy) [27]. A sample holder equipped with a thermal bath coupled to a resistive heating system was used to control the temperature of the samples during the collection of the Raman measurements (temperature stability of ± 0.1 K). The 250 nm excitation wavelength was set by regulating the undulator gap aperture and monochromatizing the incoming Synchrotron Radiation (SR) through a Czerny-Turner monochromator (750 nm focal length Acton SP2750, Princeton Instruments, Acton, MA, USA) equipped with holographic gratings with 1800 and 3600 grooves/mm. The excitation wavelength at 266 nm was provided by a CryLas FQSS 266-Q2, Diode-Pumped Passively Q196 Switched Solid-State Laser. The Raman signal of the DNA solutions was collected in back-scattered geometry, analyzed *via* a single-pass Czerny-Turner spectrometer (Trivista 557, Princeton Instruments, 750 mm of focal length) equipped with a holographic grating at 1800 g/mm and detected using a CCD camera. We collected UVRR spectra with a spectral resolution of 1.7 and 1.9 cm^{-1}/pixel for excitation wavelengths of 266 nm and 250 nm, respectively. Cyclohexane (spectroscopic grade, Sigma Aldrich) was used for calibrating the spectrometer. The final radiation power on the samples was kept between 40 and 200 μW, depending on the excitation wavelength. Continuous spinning of the sample cell during the measurements made it possible to prevent the photo-damage effect due to prolonged exposure of the sample to UV radiation. The intensity and the central wavenumber position of the Raman bands were assessed through an integration algorithm and by fitting the spectra to a suitable number of Gaussian functions after the subtraction of a flat baseline. The melting trends of the dGI and dAI Raman bands (see Results and Discussion for the definition of dGI and dAI) were fitted in the temperature range above 310-320 K using a similar two-state function [28,29] given by:

$$I(T) = \frac{C + m_C \cdot T + (D + m_D \cdot T) \cdot e^{\frac{\Delta H}{R}\left(\frac{1}{T_{G,A}} - \frac{1}{T}\right)}}{1 + e^{\frac{\Delta H}{R}\left(\frac{1}{T_{G,A}} - \frac{1}{T}\right)}} \quad (1)$$

where C and D are the lower and upper limit of the ordinate (Raman spectral band intensity), R is the gas constant, ΔH and $T_{G,A}$ are the enthalpy variation and temperature associated with the transition involving the guanine and adenine nucleobases and the parameters m_C and m_D describe the linear temperature-dependence of the intensity in the pre- and post-transition regions.

2.3. Circular dichroism and UV absorption measurements

Circular dichroism (CD) and UV absorption spectra were recorded using a Jasco J-810 polarimeter equipped with a plug-n-play single-cell Peltier with a stirrer for temperature control. We measured the samples of dsDNA in Tris buffer and Tris/DES solutions at the same concentrations used for UVRR experiments. All the solutions were freshly prepared in a rectangular quartz cell with a 1 mm path length. Each CD and UV spectrum was collected in the range from 200 to 320 nm with an increment of 1 nm, a 50 nm/min scan rate, and a 1 nm bandpass. Measurements were performed under a constant nitrogen flow, and the spectra were averaged from 4 scans. For each set of temperature-dependent measurements, the spectra of the buffer alone (Tris and Tris/DES solution) were subtracted from the corresponding samples. The CD and UV absorption melting curves were fitted to a simple two-state transition equation to calculate the dsDNA transition temperatures.

2.4. Molecular dynamics simulations

For the DESs and DNA duplex, a General Amber Force Field (GAFF) [30,31] and AMBER99SB-ILDN protein, nucleic AMBER94 [32] were used, respectively. In this work, HBD molecules, HBA molecules, and 58 sodium molecular anions to neutralize the DNA were added randomly to reach the desired DES concentration (0.154 M) in a cubic box (12.7 nm × 12.7 nm × 12.7 nm). In the second step, the simulation boxes were solvated with water molecules using the TIP3P water model [30].

The package Packmol was used for the random distribution of the salts in the simulation boxes [30,31]. After randomly adding DES and water molecules to the systems, undesirable interactions could arise. To eliminate all unfavourable interactions, the steepest descent minimization approach was utilized. Next, all systems were equilibrated by performing 100 ps of NVT (canonical ensemble) restrained simulations followed by 100 ps of NPT (isothermal–isobaric ensemble). As part of the equilibration process, a linear constraint solver (LINCS) algorithm [30] was employed for all hydrogen atom bonds, and all short-range non-bonded interactions were cut off by 1.2 nm. It should be mentioned that the particle mesh Ewald method [30] was used to treat long-range electrostatic interactions and that a Maxwell–Boltzmann distribution was used for all the simulations to produce initial velocities. In addition, a velocity-rescaling coupling algorithm was used [30] with a coupling constant of 0.1 ps to ensure constant temperature and pressure during the simulations. MD production runs were performed in an NPT ensemble for 100 ns at 300 K in which a 2-fs time step was used. In this work, MD simulations were performed using the package Gromacs 2018 [30-34]. Visual Molecular Dynamics (VMD) was also used for visualization and snapshot preparation [30]. After the simulation, some strategies including a radial distribution function (RDF) and root mean square deviation (RMSD) were performed to extract relevant information about the system. In detail, the RDF is used to describe the distribution of solvent molecules around one specific molecule or atom. The RMSD is computed to show the deviations of the backbone atoms of dsDNA from its initial structure and to represent how structures and parts of structures alter over time as compared to the starting point. Furthermore, the number of hydrogen bonds over time was calculated based on two geometric criteria: the distance between the donor and acceptor (which in Gromacs is 3.5 Å), and the angle between the hydrogen donor and acceptor (which is 30°).

3. RESULTS AND DISCUSSION

3.1. Thermal stability of double-stranded DNA in hydrated DES. Fig. 1 shows the temperature evolution of the absorbance maximum at ~260 nm for dsDNA dissolved in aqueous Tris buffer and different types of hydrated DES. The increase in the UV absorption of DNA marks a structural transition that significantly changes the extent of base stacking in the structure of dsDNA, in turn reflected by the increment of the extinction coefficient [35,36]. The variation in absorbance A_{260} observed for dsDNA in Tris buffer (Fig. 1) indicates a single relatively sharp transition with a midpoint (melting temperature, T_m) corresponding to about 331 K. The effect of the addition of DES on the melting curves of dsDNA is clearly detectable as an increase in the melting temperature T_m up to about 345 K, which was observed at the highest concentration of DES (Fig. 1).

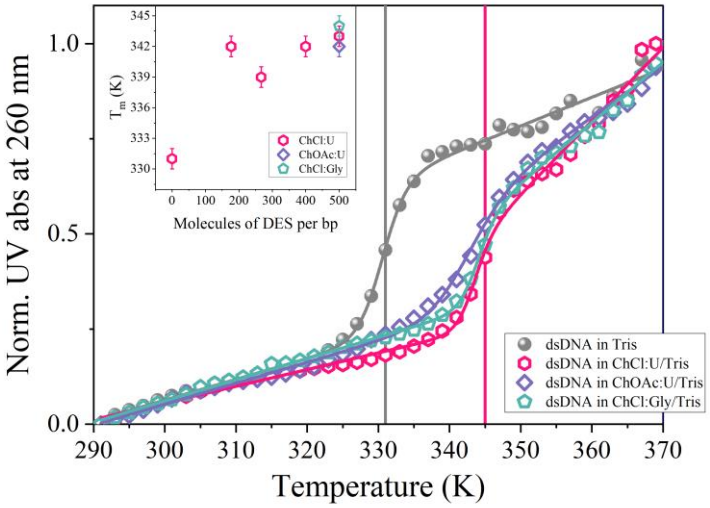

Figure 1: Temperature-dependent absorbance measured at 260 nm for dsDNA (10 μM) dissolved in Tris buffer and in hydrated DESs, i.e. ChCl:U, ChOAc:U, and ChCl:Gly 500 molecules of DES for DNA bp; full lines are fitting of experimental data with two-state transition equation. The vertical lines indicate the melting temperatures observed for dsDNA in the Tris solution (ca. 331 K) and DES solutions (ca. 345 K). Inset: Melting temperature T_m estimated by UV absorption curves for dsDNA dissolved in DES/Tris solution as a function of the number of DES per one DNA base-pair (bp).

This finding provides the first evidence that hydrated reline is able to protect the secondary structure of DNA by significantly increasing the temperature at which the dissociation of the two strands of DNA occurs [17,23,24,37]. The values of T_m reported in the inset of Fig. 1 demonstrate that the stabilization effect produced by ChCl:U DES seems to start even at a relatively low concentration of DES in water, i.e. 177 molecules of DES for each DNA base pair. We note that the increase in the T_m of DNA is substantially the same for all three of the DES considered in this study (see inset of Fig. 1).

Fig. 2(a) and (b) show the temperature-dependent CD spectra collected for dsDNA dissolved in Tris buffer and in hydrated reline, respectively.

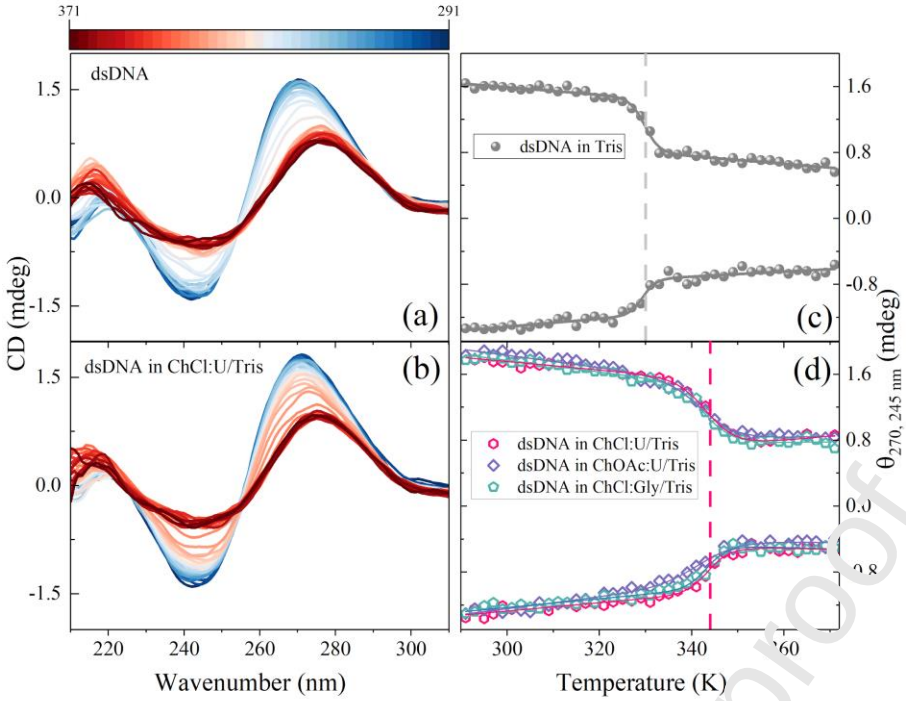

Figure 2: (a)-(b) Temperature evolution of CD spectra for dsDNA in Tris (10 μM) and in ChCl:U/Tris (molar ratio DES:bp corresponding to 500:1). (c)-(d) CD melting curves monitored at 270 (curves on top) and 245 (down) nm for dsDNA in Tris and in different DES/Tris solutions; full lines are fitting of experimental data to a two-state transition equation.

By using circular dichroism, we can efficiently probe the topology changes of dsDNA as a function of temperature by following the spectral changes in the spectroscopic signatures of the double-strand structure of DNA [28]. The CD spectra confirmed that, even at a high DES concentration in solution (molar ratio DES:bp corresponding to 500:1), the double structure of DNA is preserved over the whole explored temperature range [31]. In all cases, the characteristic CD profile of double-stranded B-form DNA, consisting of a positive and a negative band at about 270 and 245 nm respectively, is clearly distinguishable. The positive feature relates to π-π base stacking, while the negative band is associated with the polynucleotide helicity of the double-strand structure of DNA. The CD profiles in Fig. 2(b) do not show the typical marks associated with intercalation phenomena [38]. This finding corroborates the experimental results of Wang *et al.* [39], according to which dsDNA retains its inherent B-conformation in DES solutions.

The temperature evolution of the CD spectra of DNA can be quantitatively monitored by evaluating the ellipticity θ_λ at 245 and 270 nm in the explored temperature range. For dsDNA dissolved in pure Tris buffer, we note a depletion of the amplitude of the ellipticity at 270 nm and a corresponding increase in the negative band at 245 nm upon increasing the thermal motion (Fig. 2(c)). The melting curves reported in Fig. 2(c) are consistent with a general weakening of the stacking interactions between neighbouring bases and loss of the helicity in dsDNA upon the increase in temperature [28]. The change in ellipticity is monophasic and cooperative for both of the considered wavelengths, with the two transitions centered at about 329-330 K (see Table S1 in SI). When DES is added to a solution of dsDNA, a significant increase in the thermal stability of the double helix occurs, as shown by the ellipticity trends reported in Fig. 2(d). The increase of about 10 K detected for the transition temperature in the CD curves is consistent with the stabilizing effect produced by DES on the double-stranded structure of DNA as discussed above.

Noticeably, all DESs considered in this study lead to a comparable effect on the thermal stability of DNA. Both choline derivatives used in this study, i.e. ChCl and ChOAc, seem to act as the main

factor responsible for the higher T_m and T_{CD} values observed for dsDNA (see Table S1 and S2 in SI). This finding is consistent with our recent results on large molecules of DNA dissolved in hydrated DES [37]. The capability of choline ions to stabilize dsDNA by reducing the repulsive forces between the phosphate groups of the DNA strands has already been reported [23,24]. In particular, it has been shown that choline ions bind to the DNA duplex more effectively than sodium ions [23]. As a double-check, when dsDNA is dissolved in urea/Tris solution, the transition temperature only slightly increases compared to dsDNA in pure Tris buffer (see Table S1 and S2). Similar behaviour was also found for the other HBD considered in this study: Gly (see Table S1 and S2). It has been reported that low-molecular-weight co-solutes, such as glycerol, tend to destabilize dsDNA as their concentration in solution rises [40,41]. Our CD and UV absorption results may suggest that both urea and Gly are mainly excluded from the immediate vicinity of the DNA backbone, whose surface is preferentially hydrated by water molecules [41-42]. This may explain the predominant role played by the choline-based HBA species to drive the stabilization of dsDNA in hydrated DES.

3.2 Temperature dependence of UV Resonance Raman spectra of dsDNA in hydrated DES. Compared to non-resonant Raman, UVRR spectroscopy provides simplified Raman spectra of DNA with selective enhancement of some of the vibrational bands assigned to the single nucleic bases. This is related to the resonance effect achievable thanks to the slightly different UV absorption patterns of the nucleobases [45,44]. In our previous works [28,29], we have already demonstrated that selective enhancement of the Raman signals attributed to adenine dA and guanine dG vibrations in the spectra of DNA by suitable tuning the excitation wavelength.

Fig. 3(a)-(b) shows the temperature-dependent UVRR spectra of dsDNA dissolved in ChCl:U/Tris solution collected by using 250 nm and 266 nm as excitation wavelengths. Such wavelengths are very close to the absorption maximum of dG and dA nucleobases, respectively (see panel at the top in Fig. 3). Both the 250 nm- and 266 nm-excited spectra reported in Fig. 3(a)-(b) provide evidence of the effects of DES on the thermally-induced structural transitions of dsDNA that are reflected by the spectral changes detected for specific Raman markers.

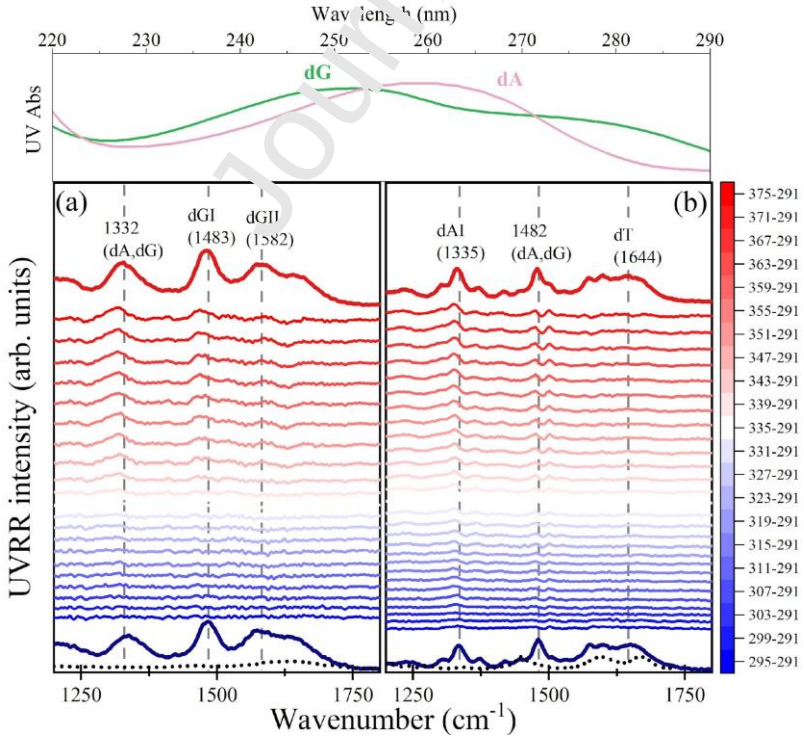

Figure 3: 250 nm- (a) and 266 nm-excited (b) Raman spectra of dsDNA 10 μM in ChCl:U/Tris solution collected at 291 K (bottom trace) and 375 K (top trace); intermediate traces are the difference spectra after subtracting the spectrum measured at the lowest temperature from the spectrum at the indicated temperatures. The spectra of ChCl:U/Tris solution at the same excitation wavelengths are also reported (dashed lines). Top panel: UV absorbance spectra of 2′-deoxyguanosine 5′- triphosphate trisodium salt solution (dG) and 2'-deoxyadenosine 5′- triphosphate sodium salt solution (dA) in Tris buffer measured at room temperature.

In the UVRR spectra reported in Fig. 3(a), the main Raman bands assigned to dsDNA are easily detectable, while the vibrational contribution arising from the solvent – the hydrated DES – is practically negligible. In the 250 nm-excited spectra of DNA, the resonance Raman profile is mostly dominated by the vibrational bands associated with guanine bases [43-45]. Specifically, we can distinguish the following bands: i) dGI ~1483 cm^{-1} attributed to N7=C8 and C8-N9 ring stretching coupled with C8-H in-plane deformation of the dG purine group, ii) dGII ~1582 cm^{-1} assigned to N3-C4, C4-C5 and C5-N7 stretching motions [43-48], and iii) the broad band at ~1332 cm^{-1} deriving from the overlap of base-ring vibrations assigned to adenine dA and guanine dG residues (for the numbering of atoms of nucleobases, see Fig. S2 in SI). These vibrations are sensitive markers of the structural changes occurring in nucleic acids, such as base unstacking and alterations in the H-bonding at the ring sites of nucleobases [44,45]. As depicted by the difference spectra reported in Fig. 3(a), upon the increase in temperature, the UVRR spectra of DNA exhibit several intensity and frequency changes of the Raman bands at ~1332, 1483, and 1582 cm^{-1}. Similarly, the 266 nm-excited UVRR spectra of dsDNA reported in Fig. 3(b) provide specific information on the ring vibrational bands assigned to the adenine dA and thymine dT residues in dsDNA [28,43]. We observed temperature-dependent changes in the intensity and frequency of some signals in the spectra of dsDNA collected using 266 nm as the excitation wavelength. In more detail, the Raman band at ~1335 cm^{-1} (dAI) is sensitive to the changes in H-bonds at the N7 acceptor site of adenine being attributed to the coupled stretching vibrations of N7=C8 and C5-N7 bonds [43,48, 51-54] (for the numbering of atoms of nucleobases see Fig. S2 in SI). The signal at ~1482 cm^{-1} is the overlapping of the contribution arising from both dA and dG residues [28]. Finally, the band labelled as dT ~1644 cm^{-1} is attributed to the stretching of C4=O and C5=C6 bonds of the thymine residue [55-57], and it is a highly sensitive marker of perturbations at the C=C site.

Figure 4(a)-(b) compares the temperature evolution of the intensity of dGI~1483 cm^{-1} and dAI~1335 cm^{-1} bands of dsDNA dissolved in Tris and ChCl:U/Tris solution.

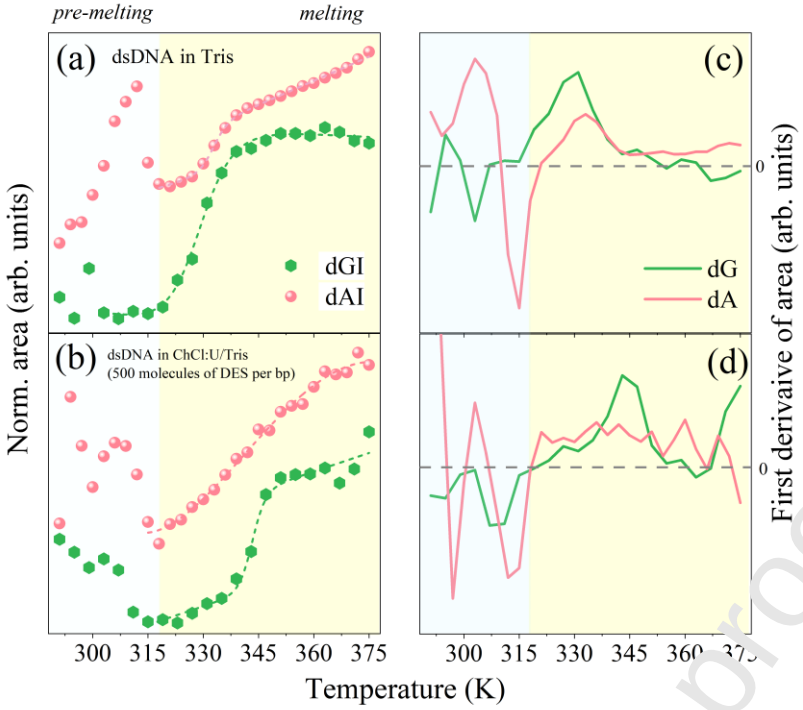

Figure 4: Melting profile for Raman bands dGI and dAI of dsDNA 10 μM in Tris (a) and ChCl:U/Tris solution (b); the trends have been normalized to their minimum and maximum values for a better comparison. Panels (c)-(d) show the corresponding temperature first derivative of profiles (a) and (b) respectively.

Fig. 4(a) shows the complex temperature dependence of the integrated intensity of both dGI and dAI for dsDNA in Tris buffer. Two main temperature regimes can be defined: *i*) a pre-melting region up to ca. 315 K. This region is characterized by temperature-dependent structural changes – observable from the Raman spectrum – occurring before the onset of the strand separation of DNA (i.e. below the melting temperature). ii) A melting range above 330 K in which a pronounced intensity increase in some of the Raman bands can be detected (Raman hyperchromicity). Thermally-induced changes in the intensity of Raman bands reflect structural modifications of the DNA subgroups to which these Raman signals are assigned [51]. In particular, the intensity variation of the Raman bands dGI and dAI has been related to the partial disruption of the vertical base-base stacking interactions (unstacking interactions) or to some reversible rearrangements such as the rupture or the weakening of H-bonds as well as bases tilting [50,58], specifically involving guanine and adenine residues. Fig. 4(a) shows, in the pre-melting region, reversible intensity variations leading to local maxima at ~299 K for dGI and ~311 K for dAI. There were no patterns in the temperature trend of UV absorbance of dsDNA at 260 nm in the pre-melting region that corresponded to these oscillations in the Raman cross section (Fig. 1). This suggests that the pre-melting features observed in Fig. 4(a) for both dGI and dAI bands can be related to a sequence of thermally-induced structural changes [28,29,59] which do not involve the complete unstacking of dG and dA bases that accompanies the dissociation of the DNA strands. The pre-melting transition monitored by the dGI band has been associated with a rearrangement of the backbone helical geometry and of the inter-guanine interactions that precede the melting of DNA [51,55,56,60,61]. Similarly, the peak in the Raman intensity of dAI band resembles pre-melting phenomena observed at room temperature for Poly (dA–dT) poly (dA–dT) double-helical B DNA [51,55,57] and in the chromosomal *calf thymus* DNA [62]. This local transformation can be connected to the establishment, even at low temperatures, of a third hydrogen bond cross-strand between consecutive dA - dT pairs that perturbs the conformations of the duplex phosphodiester backbone of DNA without significant unstacking or dissociation of the double helix. Fig. 4(b) provides evidence that the presence of DES in the DNA solution affects the pre-melting fluctuations involving guanine and adenine bases.

The trends of both dGI and dAI band intensity in the melting region of Fig. 4(a) reveal a monotonic increase above about 330 K. The observed Raman hyperchromicity finds a correspondence in the marked increase in the extinction coefficient of the UV absorption curves of DNA (Fig. 1). This finding suggests that the increase in the dGI and dAI bands can be directly related to the thermally-induced disruption of stacking interactions specifically involving guanine and adenine bases. The temperature-dependent behavior of these Raman bands in the melting region is considered to be typical of the two-state cooperative structural changes associated with the melting of dsDNA as detected by UV absorption and CD measurements [28,29,47,49,51,55,60]. It is noteworthy that, in contrast to UV and CD absorbance, the UV Raman cross section is informative of the unstacking specifically localized to guanine-pairs for the dGI band, and adenine for the dAI band [28]. Also, the structural changes in dsDNA in the melting region seem to be affected by the addition of DES to the solution (Fig. 4(b)). The effect of the DES can be estimated by the temperatures of the pre-melting and melting transitions detected by the Raman data. Such transition temperatures can be quickly extracted from the first-order derivative of the temperature curves of Fig. 4(a) and (b) (Fig. 4(c) and (d)). In Fig. 4(c)-(d), the values of temperature at which the first derivative changes sign identify the pre-melting transitions temperature for dG and dA bases. The maxima found in the derivative curves correspond to the inflection points of the two-step trends of Fig. 4(a)-(b) and match the temperature values estimated using the fitting procedure described in the experimental methods section. The temperature values of T_G and T_A associated, respectively, with the structural transitions at the dG and dA nucleobases are parameters that are sensitive to the microscopic effect exerted by DES at different sites in the structure of dsDNA (see Table S3 in SI).

3.3. DESs strongly perturb the hydration layer of AT pairs in dsDNA. Fig. 5 summarizes the values estimated for the pre-melting and melting transition temperatures T_A associated with adenine structural transformation for dsDNA in the presence of an increasing concentration of DES.

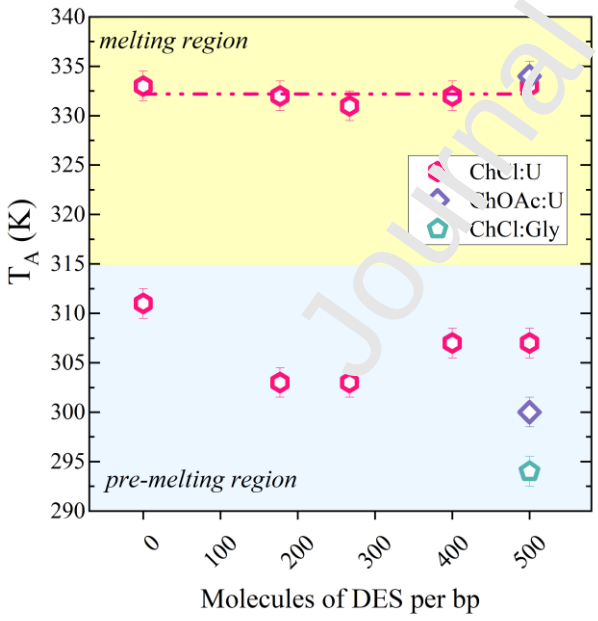

Figure 5: Effect of hydrated DES on pre-melting and melting transition temperatures localized to adenine nucleobases of dsDNA. The transition temperatures have been extracted by analysis of the band dAI~1335 cm^{-1} in the 266 nm-excited Raman spectra of dsDNA at 10 μM.

The increase in temperature is responsible for a cooperative transformation associated with a partial disruption of adenine stacking interactions that is detected for dsDNA in Tris buffer at $T_A \approx 333$ K [29] (see Table S3 in SI). T_A values in the melting region do not exhibit appreciable variations in the

presence of ChCl:U DES, even at the highest concentration explored in this study of 500 molecules of DES for each DNA base pair. The same behavior was observed for ChOAc-based DES. Similarly, the temperature dependence of the frequency position of the Raman band assigned to the dAI mode is not significantly affected by the presence of all types of DES considered in this study (see plots reported in Fig. S3 in the Supporting Information). Both these findings indicate that the presence of DES in the hydration shell of DNA mainly induces reversible base tilting rather than the rupture of hydrogen bonds or unstacking on adenine residues in dA-dT pairs [29,59]. Conversely, Fig. 5 points out that, even at the lowest concentration of ChCl:U (molar ratio DES:bp corresponding to 177:1), a depletion of at least 5 K is observed for the adenine pre-melting transition temperature compared to the case of a pristine buffer where a reversible transition is clearly detected at $T_A \approx 311$ K. Moreover, this effect appears to be further enhanced by replacing ChCl:U with ChOAc:U and ChCl:Gly. The reversible pre-melting transition associated with dA base pairs has been related to the stabilization of the extra amount of propeller twist between the A–T base planes [58] or to the disruption of the bound water in the spine of hydration in the minor groove of the duplex [42]. As already suggested by Chandran *et al.* [63], cations can penetrate the DNA hydration layers and participate in the solvation mechanisms by establishing new hydrogen bonds and favouring dA base tilting and DNA deformation [64]. This effect could explain the observed depletion of the pre-melting transition temperature for dA in the presence of DES in water. Fig. 5 shows that ChCl:U seems to affect the pre-melting transition more efficiently at low DES concentration in water; the effect is partially attenuated as the number of ChCl:U involved increases. A possible explanation may depend upon DES-DES interactions predominating over DES-DNA interactions [37] in the more concentrated DES solutions, leading to minor participation of choline ions to the solvation shell around the dA residues. Fig. 5 provides evidence that acetate-containing DES (ChOAc:U) affects the adenine pre-melting transformations more strongly than the two ChCl-based DESs. This effect is related to the fact that ChOAc:U in water undergoes breaking of DES-DES interactions more easily than ChCl:U, thus making the urea portion more prone to interact with water [65,66]. The strong solvation of urea is expected to perturb the structure of water molecules in close proximity to the DNA backbone, and this can be associated with a promotion of the local adenine pre-melting fluctuations. On the other hand, the diverse composition of DESs seems to be an important factor in modulating the effect of the solvent on DNA structure. Fig. 5 shows that replacing urea with glycerol in the ChCl-based DES leads to a lowering of the pre-melting temperature for dsDNA from about 311 to 294 K. This may suggest that Gly more strongly competes with water in the hydration spine of DNA [67] than urea, which is only able to marginally affect the orientation of water molecules in the hydration shell around the DNA backbone [41].

3.4. Preferential interaction between DES and H-bonds sites of guanine bases. Fig. 6 shows the transition temperatures T_G corresponding to the pre-melting and melting transformations specifically involving guanine bases for dsDNA in Tris and DES/Tris solution. The trends observed in Fig. 6 are complementary to those in Fig. 5. The results indicate that ChCl:U does not induce any remarkable effect on the pre-melting of dG nucleobases over all the explored concentration ranges of DES in water, but very much affects T_G. Indeed, we observe a characteristic reversible structural transition mainly localized to dG bases at a temperature of $T_G \approx 299$ K (pre-melting region) for dsDNA both in the absence and presence of ChCl:U, ChOAc:U and ChCl:Gly. This finding was in part expected, considering that the pre-melting thermal fluctuations in DNA are connected to the formation of local interbase H-bonds disrupted states in A-T base pairs with much higher probability than in the G-C pair [68,69]. However, it can also be argued that the H-bond network of water molecules in the hydration shell around guanine nucleobases is less strongly perturbed by DES components than the layer of hydration around adenine bases.

The cooperative transition detected for dsDNA at $T_G \approx 329$ K (melting region) comes from structural modifications to guanine bases associated with the helix-to-coil transition promoted by thermal motion. As clearly evident in Fig. 6, the increase in ChCl:U concentration in Tris causes a corresponding increase in the guanine melting temperature T_G from about 329 to 342 K at the highest concentration of DES considered in this study. ChOAc:U and ChCl:Gly exhibit the same effect of ChCl:U on the guanine melting transition.

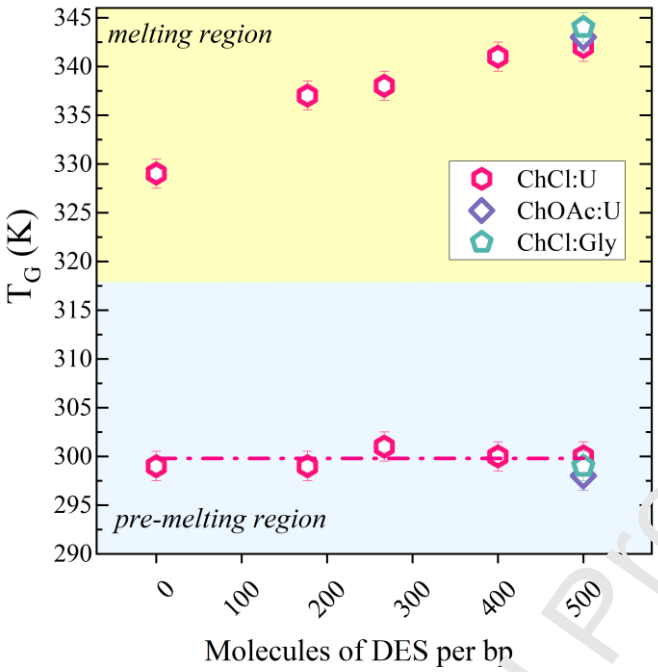

Figure 6: Effect of hydrated DES on pre-melting and melting transition temperatures localized to guanine nucleobases of dsDNA. The transition temperatures were extracted by analysis of the band dGI~1483 cm^{-1} in the 250 nm-excited Raman spectra of dsDNA at 10 μM.

The extent of T_G increase is fully consistent with the enhancement of the melting temperature observed for dsDNA in hydrated DES and experimentally detected by UV and CD melting experiments (Fig. 1 and 2). Since the UV Raman intensity of the dGI band directly probes the partial disruption of guanine stacking interactions that precedes the separation of DNA strands during melting, the increase in T_G can be explained by the formation of a preferential interaction between DES molecules and the guanine residues on DNA grooves [29,59]. The strong H-bond capability of acetate ions and urea probably contributes to the formation of a stable interaction with the N7 and C6=O sites of dG nucleobases with ChCl:U and ChOAc:U. Similarly, the hydroxyl groups of glycerol in ChCl:Gly provide further H-bond sites in which guanine bases can be involved [25]. Overall, these strong DES-DNA interactions lead to a more effective stacking between guanine bases even at high temperature values, contributing to stabilizing the double-helix structure of DNA [21,39].
In agreement with the findings of the CD experiments discussed above, we can suppose the predominance of a groove binding mechanism for the interaction between DES compounds and the DNA structure instead of intercalation phenomena.
The preferential interaction between DES and guanine bases in the DNA groove seems to be also confirmed by the temperature dependence of the frequency position of the Raman band dGI shown in Fig. 7.

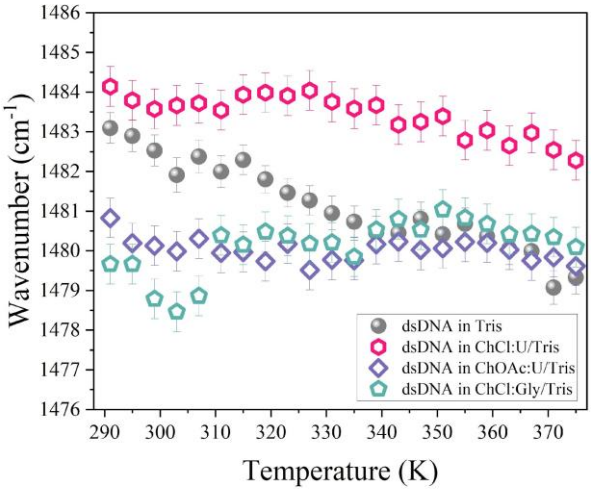

Figure 7: Temperature evolution of central wavenumber position of dGI Raman band of 10 μM dsDNA in the absence and in the presence of different types of DES (molar ratio DES:bp corresponding to 500:1).

As expected, we observe a red shift of about 4 cm^{-1} for the wavenumber position of the dGI band with increasing temperature for dsDNA in Tris [28,29,57,59]. This reflects the strengthening of H-bonds on the N7 site of guanine that has been attributed to the progressive replacement of base-base H-bonds with base-water interactions promoted by the increase in thermal motion [50]. Remarkably, Fig. 7 shows only a slight dependence on temperature of the dGI band in the presence of ChCl:U, ChOAc:U and ChCl:Gly compared to pure Tris buffer. This may confirm the preferential interactions of DES compounds toward guanine bases that, especially at high temperatures, tend to act as a competitor to water for establishing H-bonds with dG that do not significantly change the frequency of the dGI mode.

3.5. Does the anion influence the DES-dsDNA interactions? The role of interactions of the components of DESs (choline cations, chloride and acetate anions, and urea and glycerol molecular species) with dsDNA was investigated by MD simulations. As a first step, the preferred localization of the choline-DNA interactions was extracted from the MD trajectories as shown in Fig. 8(a)-(c), where the Radial distribution function (RDF) of choline around the major groove and minor groove of DNA in the aqueous solution of ChOAc:U and ChCl:U are shown in order.

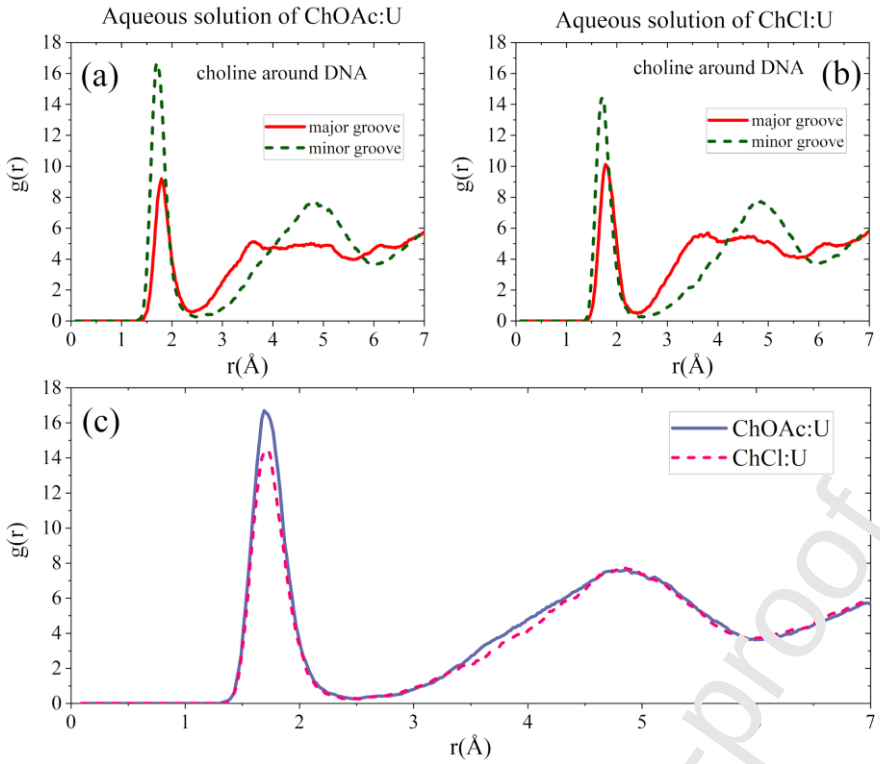

Figure 8: Radial distribution functions of choline around different parts of dsDNA, including major groove and minor groove in aqueous solution of ChOAc:U (a) and ChCl:U (b). Radial distribution functions of choline around minor groove in aqueous solution of ChOAc:U and ChCl:U (c). H site of OH group for choline, electronegative sites N3 and O2 for minor groove, and electronegative sites N7, N4, and O4 for major groove were considered for RDF calculations.

Considering Fig. 8(a) and 8(b), the MD simulations indicate that, in both solutions, choline has a sharp and intense peak at ca. 1.75-1.80 Å from the DNA groove sites, irrespective of the groove type. This means that the Ch cations do contribute significantly to the first neighbours' layer of dsDNA and are part of the first solvation shell. In the aqueous solution of ChCl:U, the minor and major grooves reach peaks at 14.45 and 3.92 at distances of 1.7 and 1.8 (Å) respectively. In the aqueous solution of ChOAc:U, the minor and major grooves reach peaks at 16.76 and 9.11 at distances of 1.7 and 1.8 (Å) respectively. The intensity of the peaks corresponding to the minimum Ch-DNA distance is significantly different in the minor groove and major groove (dashed and continuous lines in Fig. 8(a) and 8(b), respectively). This is a clear-cut indication that the population of choline cations in the first solvation shell of dsDNA is selectively imbalanced towards the minor groove. The interaction of choline ions in minor groove of DNA is evident also by inspection of Fig. S4 in the SI displaying some representative snapshots at regular intervals of MD simulation. Incidentally, docking simulations provide further support to the selective affinity of choline to the DNA minor groove (see Fig. S5 in the SI section). In a previous investigation on the same sample of dsDNA, we observed a preferential interaction of imidazolium-based ionic liquids with the major groove [29]. In this work, the cholinium cation seems to exhibit the opposite affinity, as the preferred interaction groove is the minor one. A possible rationale may rely upon the larger steric hindrance of alkylimidazolium ions compared to cholinium species, driving the coulombic and/or H-bond interactions of the cations towards the major groove with IL, or to the minor groove with DES. This finding may be consistent with the high affinity of choline ions for the A-T base pair minor groove, previously observed by Nakano et al. [23]. This effect has been explained based on the narrower width and the more electrostatically polar character of the DNA minor groove with respect to the major one [23]. The preferential binding of choline ions with the DNA minor grooves may be responsible for the observed stabilizing effect of DES, since the choline ions can form multiple hydrogen bonds with DNA that do not disrupt base pairing [23]. RDF of Fig. 8(a) and 8(b) also indicate marked differences in the choline

distribution in the second solvation shell. Indeed, the RDF curves related to the minor groove distance (dashed curves) show in both cases (Fig. 8(a) and 8(b)) a well-defined maximum at ca. 4.75 Å, obviously broader than the one related to the first shell. Conversely, the full stretch lines in Fig. 8(a) and 8(b) do not show any structuration, with a plateau at r > 3.5 Å. This finding provides computational evidence of a selective response of dsDNA to the perturbation introduced by the DES: the minor groove is more sensitive than the major grove to the presence of choline cations in the first and second solvation shells, both in terms of population and of structural organization of the choline units around dsDNA. Finally, and only considering the distribution of choline around the minor grove (Fig. 8(c)), the distribution of choline around dsDNA is influenced by the counterion, keeping the HBD component constant (urea in the examined cases): the presence of acetate instead of chloride seems to noticeably increase the population of the choline in the first solvation shell of dsDNA.

Another important descriptor of the DES-DNA interaction can be calculated from the root-mean-square deviation (RMSD) of dsDNA atomic coordinates considering the four hydrated DESs (molar ratio DES:bp equal to 500:1) and the control case in water. The comparison of such data with the reference in pure water is shown in Table 1. The physical meaning of the curves is to quantify the effect of the DES component on the fluctuations in atomic coordinates of DNA as a function of the simulation time, keeping the temperature constant, *i.e.* the background of the thermal fluctuations (Fig. 9). Table 1 shows the average RMSD value in the aqueous solutions of ChOAc:U, ChCl:U, ChCl:Gly, and in pure water. The data on RMSD are consistent with the stabilizing effects of DES on the structure of DNA in comparison to a pure water environment.

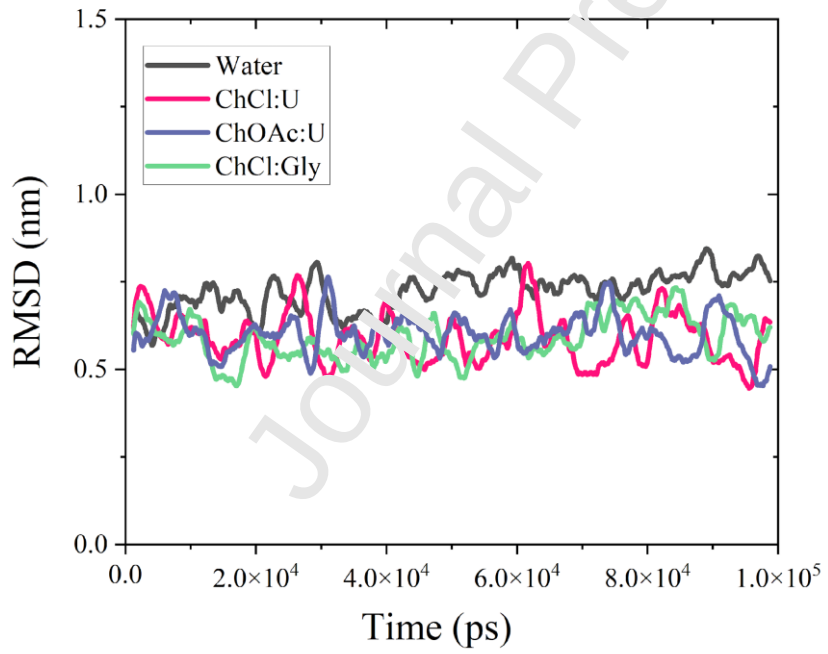

Figure 9: Root-mean-square deviation (RMSD) of dsDNA solvated in four hydrated DESs (molar ratio DES:bp corresponding to 500:1) and in pure water at 300 K as a function of time used for the simulation.

Table 1: Average RMSD value in aqueous solution of ChOAc:U, ChCl:U, ChCl:Gly, and pure water.

Solvent	Concentration (M)	Average RMSD value (nm)
Water	-	0.721
ChCl:U	0.154	0.588
ChOAc:U	0.154	0.600
ChCl:Gly	0.154	0.589
ChCl:U	0.115	0.602
ChCl:U	0.07	0.632

3.6. The effect of HBD on DES-dsDNA interactions. Fig. 10(a)-(d) show the RDFs of glycerol and urea molecules around the major groove and minor groove of DNA in the aqueous solutions of ChCl:Gly and ChCl:U. For the sake of comparison, the same calculations are also reported for 0.3 M solutions of U and Gly, corresponding to a molar ratio DES:bp of 500:1. The figures point out a preferential interaction of U and Gly with the minor groove in both cases. However, the behavior of Gly and U are different in the presence or absence of ChCl, probably as a consequence of the complex competition of HBD and HBA with water molecules. The sharp peak of Fig. 10(a) with the ordinate value largely above 1.7 Å indicates a statistically significant population of Gly undergoing a short-range interaction with the minor groove only in the absence of ChCl. Conversely, the plots of RDF of U (Fig. 10(c)) in the aqueous solutions of DES or as 0.3 M urea solution show two overlapped sharp maxima at ca. 1.95 Å. This result indicates that the first-neighbor distance statistics of U-dsDNA interactions are not influenced by the presence of ChCl. Additionally, well-defined peaks for the second, third and fourth solvation shells can be seen in Fig. 10 for both 0.3 M urea and 0.154 M ChCl:U solutions. Noticeably, no structured solvation shells beyond the first one can be observed in Fig. 10(a), with the only exception of the second maximum of 0.3 M Gly. Furthermore, the hydrogen-bond lifetime of the water molecules was calculated based on cutoffs for the angle Hydrogen - Donor - Acceptor and the distance Donor – Acceptor, which in Gromacs is 30° and 3.5 Å, respectively. According to Table 2, the hydrogen-bond lifetime of water molecules in the minor groove of DNA in the aqueous solution of ChCl:Gly, Glycerol, ChCl:U and Urea are 90.13 ps, 68.68 ps and 86.07 ps, 62.18 ps, respectively. Moreover, the energy of hydrogen bonds in the above-mentioned solutions has a similar trend as the lifetime of hydrogen bonds. The H-bond lifetime of water molecules is systematically longer in the presence of Gly compared to U. This observation confirms that glycerol and U affect the distribution of water molecules around DNA differently, potentially modulating the stability of DNA. Consistent with the variation in the pre-melting temperatures experimentally detected for adenine nucleobase (see Fig. 5 and Table S3), we can state that Gly tends to more strongly compete with water in the solvation layer of dA than urea.

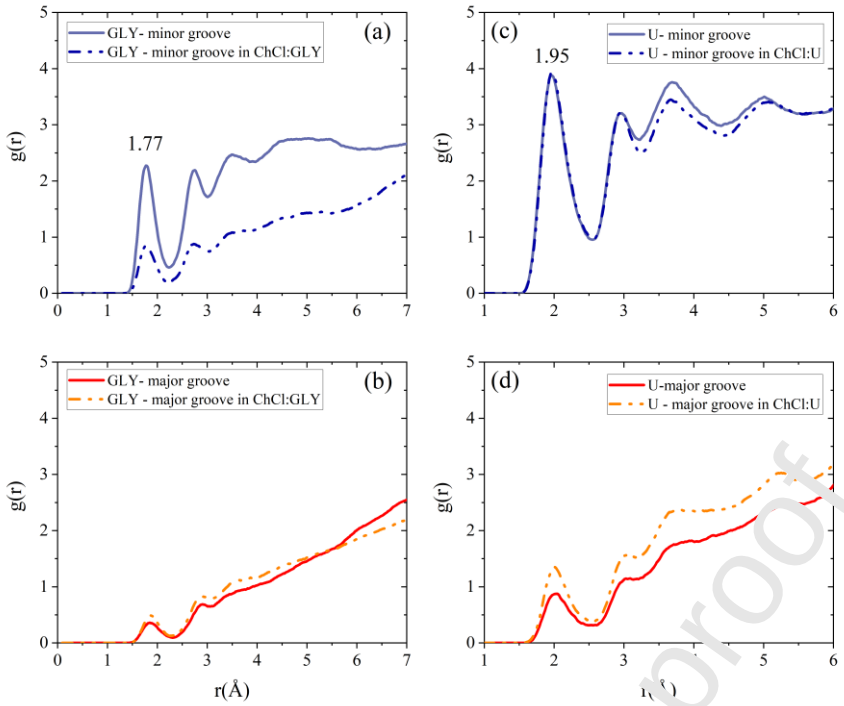

Figure 10: Radial distribution of glycerol around minor (a) and major (b) groove of dsDNA in aqueous solution of ChCl:Gly (DES:bp equal to 500:1) and in aqueous solution of Gly (DES:bp equal to 500:1). Radial distribution of urea around minor (c) and major (d) groove of dsDNA in aqueous solution of ChCl:U (DES:bp equal to 500:1) and aqueous solution of U (DES:bp equal to 500:1). The center of mass of glycerol and urea were considered for calculations of RDF.

Table 2: Hydrogen-bond lifetime of water molecules in minor and major grooves of DNA.

Solvent	Concentration (M)	Major groove (ps)	Minor groove (ps)	HB energy-major groove (KJ/mol)	HB energy-minor groove (KJ/mol)	
Urea	0.300	32.41	62.18	10.717	15.243	
Gly	0.300	34.31	68.68	11.234	15.287	
ChCl:U	0.154	40.62	86.07	13.204	16.060	
ChCl:Gly	0.154	41.26	90.13	12.353	16.359	

3.7. The effect of concentration of DESs on the stability of DNA. Fig. 11 shows the RMSD of DNA solvated in pure water and the three different concentrations of hydrated ChCl:U. According to the RMSD graphs and the average RMSD values (Table 1) of ChCl:U at different concentrations, the amplitude of the dsDNA coordinates fluctuations decreases with increasing concentration of DES in solutions.

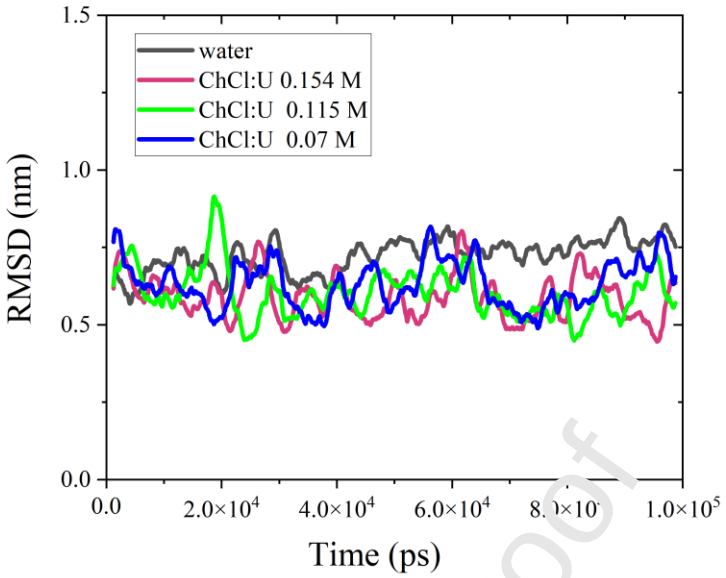

Figure 11: Root-mean-square deviation (RMSD) of dsDNA solvated in pure water and the three different concentrations of hydrated ChCl:U at 300 K as a function of time used for the simulation.

Fig. S6 (in SI) shows the concentration dependence of choline molecules around the minor groove of DNA in different aqueous solutions of ChCl:U (0.154 M, 0.115 M and 0.07 M). By increasing the concentration of DES, the probability of finding choline around the DNA minor groove decreases. This might be because of the priority of the DES-DES interactions over the involvement of choline ions in the solvation shell of DNA.

4. SUMMARY AND CONCLUSIONS

The option of using DESs is attractive in the field of DNA technology due to the low cost of their constituent compounds, their simple preparation and the eco-friendly character of these neoteric solvents. In this work, we have implemented a systematic investigation of the effect of hydrated choline-based DES on the structural stability of a 30-base pair double-stranded model DNA.
Based on absorbance measurements at 260 nm, a melting temperature of about 331 K was determined for the studied perfect DNA duplex in a purely aqueous environment. In the hydrated DES, the T_m shifted to a value of about 345 K. Identical experiments were performed using CD spectroscopy to elucidate the structural details of dsDNA, especially the π-π stacking interaction and the helicity evaluation at 245 and 270 nm. Structural transitions for both wavelengths were observed at 330 K for dsDNA in the pure aqueous environment and at 343 K after its dissolution in DES. Overall, these temperature experiments indicate a significant contribution of DES to the stabilization of the double-stranded canonical (B-form) DNA structure, even at a relatively low concentration of DES in water.
Structural dynamics insights were further evaluated using SR-UVRR measurements as a function of temperature changes. Some Raman bands associated with vibrations localized on guanine and adenine residues are selectively enhanced in the Raman spectra collected at the excitation wavelengths in resonance with the absorption maxima of these nucleobases. The spectral parameters of these vibrational bands reflect structural (intramolecular) changes and also extra-molecular DNA solvent interactions. In addition, SR-UVRR is used to monitor not only purely thermal denaturation (melting) but also pre-melting structural transitions occurring in the DNA duplex. Using different DES/DNA bp ratios, it was shown that the dA vibrational band marks a change in the pre-melting transformation

involving adenine (T_A~300 K), and not in the melting one for all studied DES. The results indicate that the hydration of AT pairs is perturbed in the presence of DES. The opposite trend was observed for the dG vibrational band, which probes a structural transition at T_G = 345 K, fully corresponding with the T_m determined by absorption and CD measurements. These results show that the interactions of guanine residues are significantly involved in the stabilization of the dsDNA structure in the presence of DES. This is mainly ascribed to the establishment of an interaction between N7=C8 and C8-N9 H-bond sites of guanine residues and DES. In addition to experimental results, MD calculations confirmed the preferential binding of DES compounds to the minor groove of dsDNA. Specifically, the RDF (used to describe the distribution of the solvent in proximity of the DNA molecule) showed, for the first and subsequent solvation layers, that the minor groove is significantly selective for the choline part of the investigated DESs compared to the major groove. A higher affinity for the minor groove than for the major groove was also confirmed for HBD components, specifically for Gly and U. This finding is likely to have a significant impact not only in terms of thermal stability, but also in the modulation of ligand-DNA interactions.

ACKNOWLEDGMENTS

We gratefully acknowledge Elettra Sincrotrone Trieste for providing access to its synchrotron radiation facilities and for financial support. The authors gratefully acknowledge the CERIC-ERIC Consortium for access to experimental facilities and financial support. BM would like to acknowledge the supply of computational resources by the project "e-Infrastruktura CZ" (e-INFRA CZ LM2018140) supported by the Ministry of Education, Youth and Sports of the Czech Republic and grant GAČR 21-15936S from the Czech Science Foundation. MT wishes to thank the European Regional Development Fund and Interreg V-A Italy Austria 2014–2020 through the Interreg Italy-Austria project ITAT 1059 InCIMa4 ‘‘InCIMa for Science and SMEs”. AM would like to thank Politecnico di Milano for granting a one-year sabbatical at Elettra Sincrotrone.

References

[1] T. Lindahl, B. Nyberg, Rate of depurination of native deoxyribonucleic acid, Biochemistry 11(19) (1972) 3610–3618, https://doi.org/10.1021/bi00769a018.

[2] J. Cadet, T. Delatour, T. Douki, D. Gasparutto, J.-P. Pouget, J.-L. Ravanat, S. Sauvaigo, Hydroxyl radicals and DNA base damage, Mutat. Res./Fundam. Mol. Mech. Mutagen. 424 (1-2) (1999) 9–21, https://doi.org/10.1016/S0027-5107(99)00004-4

[3] V.A. Sorokin, G.O. Gladchenko, V.A. Valeev, I.V. Sysa, L.G. Petrova, Yu.P. Blagoi, Effect of salt and organic solvents on DNA thermal stability and structure, J. Mol. Struct. 408/409 (1997) 237-240, https://doi.org/10.1016/S0022-2860(96)09711-6

[4] J. R. De Xammar Oro, J. R. Grigera, On the Thermal Stability of DNA in Solution of Mixed Solvents, J. Biol. Phys. 21 (1995) 151-154, https://doi.org/10.1007/BF00712343

[5] S. Nakano, N. Sugimoto, The structural stability and catalytic activity of DNA and RNA oligonucleotides in the presence of organic solvents, Biophys. Rev. 8 (2016) 11–23 https://doi.org/10.1007/s12551-015-0188-0

[6] G.Bonner, A. M. Klibanov, Structural Stability of DNA in Nonaqueous Solvents, Biotechnol. Bioeng., 68 (2000) 339-344, https://doi.org/10.1002/(SICI)1097-0290(20000505)68:3<339::AID-BIT12>3.0.CO;2-O

[7] S. A. Markarian, A. M. Asatryan, K. R. Grigoryan, H. R. Sargsyan, Effect of diethylsulfoxide on the thermal denaturation of DNA, Biopolymers 82 (2006) 1–5, https://doi.org/10.1002/bip.20454

[8] R. D. Blake, S. G. Delcourt, Thermodynamic effects of formamide on DNA stability, Nucleic Acids Res. 24 (1996) 2095–2103 https://doi.org/10.1093/nar/24.11.2095

[9] H. Tateishi-Karimata, N. Sugimoto, Biological and nanotechnological applications using interactions between ionic liquids and nucleic acids. Biophys. Rev., 10, (2018) 931–940, https://doi.org/10.1007/s12551-018-0422-7.
[10] R. Vijayaraghavan, A. Izgorodin, V. Ganesh, M. Surianarayanan, D. R. MacFarlane,D.R. Long-term structural and chemical stability of DNA in hydrated ionic liquids. Angew. Chem. Int. Ed., 49 (2010) 1631–1633 https://doi.org/10.1002/anie.200906610
[11] A. P Abbott, G. Capper, D. L. Davies, R. K. Rasheed, V. Tambyrajah, Novel Solvent Properties of Choline Chloride/Urea Mixtures. Chem. Commun. 1 (2003) 70−71, https://doi.org/10.1039/B210714G
[12] H. Vanda, Y. Dai,E. G. Wilson, R.Verpoorte, Y. H. Choi, Green solvents from ionic liquids and deep eutectic solvents to natural deep eutectic solvents. Comptes Rendus Chim., 21, (2018) 628–638, https://doi.org/10.1016/j.crci.2018.04.002
[13] T.E. Achkar, S. Fourmentin, H. Greige-Gerges, Deep eutectic solvents: An overview on their interactions with water and biochemical compounds. J. Mol. Liquids 288 (2019) 111028 https://doi.org/10.1016/j.molliq.2019.111028
[14] I. Gállego, M. A. Grover, N. V. Hud Folding and Imaging of DNA Nanostructures in Anhydrous and Hydrated Deep-Eutectic Solvents. Angew. Chem. Int. Ed 127 (2015) 6869–6873. https://doi.org/10.1002/anie.201412354
[15] H. Tateishi-Karimata, N. Sugimoto, Structure, stability and behaviour of nucleic acids in ionic liquids Nucleic Acid Res. 42(14) (2014)8831–8844 doi: https://doi.org/10.1093/nar/gku499
[16] S. Pal, S. Paul, Effect of Hydrated and Nonhydrated Choline Chloride−Urea Deep Eutectic Solvent (Reline) on Thrombin-Binding G-quadruplex Aptamer (TBA): A Classical Molecular Dynamics Simulation Study. J. Phys. Chem. C 123 (2019) 11686−11698 https://doi.org/10.1021/acs.jpcc.9b01111
[17] S. Pal, S. Paul, Understanding The Role of Reline, a Natural DES, on Temperature- Induced Conformational Changes of C-Kit G-Quadruplex DNA: A Molecular Dynamics Study. J. Phys. Chem. B 124 (2020) 3123−3136 https://dx.doi.org/10.1021/acs.jpcb.0c00644
[18] G. Sharma, R. Alphons Sequeira, M. M. Pereira, T. Kumar Maity, N. A. Chudasama, K. Prasad, Are ionic liquids and deep eutectic solvents the same?: Fundamental investigation from DNA dissolution point of view. J. Mol. Liq. 328 (2021) 115386 https://doi.org/10.1016/j.molliq.2021.115386
[19] C. Zhao, X. Qu, Recent progress in G-quadruplex DNA in deep eutectic solvent. Methods 64(1) (2103) 52-58 https://doi.org/10.1016/j.ymeth.2013.04.017
[20] R. Svigelj, N. Dossi, C. Grazioli, R. Toniolo, Deep Eutectic Solvents (DESs) and Their Application in Biosensor Development. Sensors 21 (2021) 4263. https://doi.org/10.3390/s21134263
[21] I. Mamajanov, A.E Engelhart, H.D. Bean, N.V. Hud, DNA and RNA in anhydrous media: Duplex, triplex, and G-quadruplex secondary structures in a deep eutectic solvent. Angew. Chem. Int. Ed. 49 (2010) 6310–6314 https://doi.org/10.1002/anie.201001561
[22] H. Zhao, DNA stability in ionic liquids and deep eutectic solvents. J. Chem. Technol. Biotechnol. 90 (2015) 19–25 https://doi.org/10.1002/jctb.4511
[23] M. Nakano, H. Tateishi-Karimata, S. Tanaka, N. Sugimoto, Choline Ion Interactions with DNA Atoms Explain Unique Stabilization of A–T Base Pairs in DNA Duplexes: A Microscopic View. J. Phys. Chem. B 118 (2014) 379–389 https://doi.org/10.1021/jp406647b
[24] D. Mondal, M. Sharma, C. Mukesh, V. Gupta, K. Prasad, Improved solubility of DNA in recyclable and reusable bio-based deep eutectic solvents with long-term structural and chemical stability. Chem. Commun. 49 (2013) 9606–9608 https://doi.org/10.1039/C3CC45849K
[25] R. Yusof, K. Jumbri, H. Ahmad, E. Abdulmalek, M.B. Abdul Rahman, Binding of tetrabutylammonium bromide based deep eutectic solvent to DNA by spectroscopic analysis. Spectrochim. Acta - Part A Mol. Biomol. Spectrosc. 253 (2021) 119543 https://doi.org/10.1016/j.saa.2021.119543
[26] C. Ma, A. Laaksonen, C. Liu, X. Lu, X. Ji, The peculiar effect of water on ionic liquids and deep eutectic solvents. Chem. Soc. Rev. 47 (2018) 8685–8720 https://doi.org/10.1039/C8CS00325D
[27] B. Rossi, C. Bottari, S. Catalini, A. Gessini, F. D'Amico, C. Masciovecchio, Synchrotron based UV Resonant Raman scattering for material science, in V. P. Gupta, Y. Ozaki (Eds.), Molecular and Laser Spectroscopy, Elsevier: Amsterdam, The Netherlands, 2020; Chapter 13; Volume 2, pp. 447–478.

[28] C. Bottari, S. Catalini, P.Foggi, I. Mancini, A. Mele, D.R. Perinelli, A. Paciaroni, A. Gessini, C. Masciovecchio, B. Rossi, Base-specific pre-melting and melting transitions of DNA in presence of ionic liquids probed by synchrotron-based UV resonance Raman scattering. J. Mol. Liq. 330 (2021) 115433 https://doi.org/10.1016/j.molliq.2021.115433
[29] F. Fadaei, M. Tortora, A. Gessini, C. Masciovecchio, S. Catalini, J. Vigna, I. Mancini, A. Mele, J. Vacek, D. Reha, B. Minofar, B. Rossi, Structural specificity of groove binding mechanism between imidazolium-based ionic liquids and DNA revealed by synchrotron-UV Resonance Raman spectroscopy and molecular dynamics simulations. J. Mol. Liq. 347 (2022) 118350 https://doi.org/10.1016/j.molliq.2021.118350
[30] D. A. Case, T. A. Darden, T. E. Cheatham, C. L. Simmerling, J. Wang, R.E. Duke, P. A. Kollman, (2008) Amber 10 (No. BOOK). University of California
[31] K.G. Sprenger, V.W. Jaeger, J. Pfaendtner, The general AMBER force field (GAFF) can accurately predict thermodynamic and transport properties of many ionic liquids, J. Phys. Chem. B 119 (18) (2015) 5882–5895 https://doi.org/10.1021/acs.jpcb.5b00689
[32] Lindorff-Larsen, K.; Piana, S.; Palmo, K.; Maragakis, P.; Klepeis, J.L.; Dror, R.O.; Shaw, D.E. Improved side-chain torsion potentials for the Amber ff99SB protein force field. Proteins 78 (2010) 1950–1958 https://doi.org/10.1002/prot.22711
[33] Jorgensen, W.L.; Chandrasekhar, J.; Madura, J.D.; Impey, R.W.; Klein, M.L. Comparison of simple potential functions for simulating liquid water. J. Chem. Phys. 79 (1983) 926–935 https://doi.org/10.1063/1.445869
[34] J.M. Martínez, L. Martínez, Packing optimization for automated generation of complex system's initial configurations for molecular dynamics and docking, J. Comput. Chem. 24 (7) (2003) 819–825 https://doi.org/10.1002/jcc.10216
[35] I. Tinoco, Hypochromism in polynucleotides, J. Am. Chem. Soc. 82 (1960) 4785-4790 https://doi.org/10.1021/ja01503a007
[36] W. Rhodes, Hypochromism and other spectral properties of helical polynucleotides, J. Am. Chem. Soc. 83 (1961) 3609-3617 https://doi.org/10.1021/ja01478a017
[37] M. Tortora, J. Vigna, I. Mancini, A. Mele, A. Gessini, C. Masciovecchio, B. Rossi, Effect of Hydrated Deep Eutectic Solvents on the Thermal Stability of DNA. Cryst. 11 (2021) 1057 https://doi.org/10.3390/cryst11091057
[38] S. Parodi, F. Kendall, C. Nicolini. A clarification of the complex spectrum observed with the ultraviolet circular dichroism of ethidium bromide bound to DNA. Nucleic Acids Res. 2 (1975) 477–486 https://doi.org/10.1093/nar/2.4.477
[39] N. Li, Y. Wang, K. Xu, Q. Wen, X. Ding, H. Zhang, Q. Yang, High-performance of deep eutectic solvent based aqueous bi-phasic systems for the extraction of DNA. RSC Adv. 6 (2016) 84406–84414. https://doi.org/10.1039/C6RA17689E
[40] L. J. Nordstrom, C. A. Clark, B. Andersen, S. M. Champlin, J.J. Schwinefus, Effect of ethylene glycol, urea, and *N*-methylated glycines on DNA thermal stability: The role of DNA base pair composition and hydration. Biochemistry 45 (2006) 9604–9614. https://doi.org/10.1021/bi052469i
[41] E. A. Oprzeska-Zingrebe, J. Smiatek, Preferential Binding of Urea to Single-Stranded DNA Structures: A Molecular Dynamics Study. Biophys. J. 114 (2018) 1551–1562. https://doi.org/10.1016/j.bpj.2018.02.013
[42] C. H. Spink, J. B. Chaires, Effects of hydration, ion release, and excluded volume on the melting of triplex and duplex DNA. Biochemistry 38 (1999) 496–508. https://doi.org/10.1021/bi9820154
[43] S.P.A. Fodor, R.P. Rava, T.R. Hays, T.G. Spiro, Ultraviolet resonance Raman spectroscopy of the nucleotides with 266-, 240-, 218-, and 200-nm pulsed laser excitation, J. Am. Chem. Soc. 107 (6) (1985) 1520–1529, https://doi.org/10.1021/ja00292a012
[44] S.P.A. Fodor, T.G. Spiro, Ultraviolet resonance Raman spectroscopy of DNA with 200–266-nm laser excitation, J. Am. Chem. Soc. 108 (12) (1986) 3198–3205 https://doi.org/10.1021/ja00272a006
[45] F. Bianchi, L. Comez, R. Biehl, F. D'Amico, A. Gessini, A.M. Longo, C. Masciovecchio, C. Petrillo, A. Radulescu, B. Rossi, F. Sacchetti, F. Sebastiani, N. Violini, A. Paciaroni, Structure of human telomere G-quadruplex in the presence of a model drug along the thermal unfolding pathway, Nucleic Acids Res. 46 (22) (2018) 11927–11938 https://doi.org/10.1093/nar/gky1092.

[46] Z.Q. Wen, G.J. Thomas Jr., UV resonance Raman spectroscopy of DNA and protein constituents of viruses: assignments and cross sections for excitations at 257, 244, 238, and 229 nm, Biopolymers 45 (5) (1998) 247–256 https://doiorg/10.1002/(SICI)1097-0282(199803)45:3<247::AID-BIP7>3.0.CO;2-R.
[47] P.Y. Turpin, L. Chinsky, A. Laigle, B. Jollès, DNA structure studies by resonance Raman spectroscopy, J. Mol. Struct. 214 (1989) 43–70 https://doi.org/10.1016/0022-2860(89)80005-5
[48] S.S. Chan, R.H. Austin, I. Mukerji, T.G. Spiro, Temperature-Dependent Ultraviolet Resonance Raman Spectroscopy of the Premelting State of dA* dT DNA, Biophys. J. 72 (4) (1997) 1512–1520 https://doi.org/10.1016/S0006-3495(97)78799-X.
[49] J.G. Duguid, V.A. Bloomfield, J.M. Benevides, G.J. Thomas Jr., Raman Spectroscopy of DNA-Metal Complexes. I. The Thermal Denaturation of DNA in the Presence of Sr^{2+}, Ba^{2+}, Mg^{2+}, Ca^{2+}, Mn^{2+}, Co^{2+}, Ni^{2+}, and Cd^{2+}, Biophys. J. 69 (1995) 2623–2641 https://doi.org/10.1016/S0006-3495(95)80133-5
[50] J.G. Duguid, V.A. Bloomfield, J.M. Benevides, G.J. Thomas, DNA melting investigated by differential scanning calorimetry and Raman spectroscopy, Biophys. J. 71 (6) (1996) 3350–3360 https://doi.org/10.1016/S0006-3495(96)79528-0.
[51] L. Movileanu, J.M. Benevides, G.J. Thomas Jr, Temperature Dependence of the Raman Spectrum of DNA. Part I—Raman Signatures of Premelting and Melting Transitions of Poly(dA–dT)_Poly(dA–dT), J. Raman Spectrosc. 30 (1999) 637– 649 https://doi.org/10.1002/(SICI)1097-4555(199908)30:8<637::AIDJRS431>3.0.CO;2-B
[52] J.M. Benevides, S.A. Overman, G.J. Thomas, Raman, polarized Raman and ultraviolet resonance Raman spectroscopy of nucleic acids and their Complexes, J. Raman Spectrosc. 36 (4) (2005) 279–299 https://doi.org/10.1002/jrs.1324
[53] N. Fujimoto, A. Toyama, H. Takeuchi, Effects of hydrogen bonding on the UV resonance Raman bands of the adenine ring and its C8-deuterated analog, J. Mol. Struct. 447 (1-2) (1998) 61–69 https://doi.org/10.1016/S0022-2860(98)00301-9
[54] A. Toyama, H. Takeuchi, I. Harada, Ultraviolet resonance Raman spectra of adenine, uracil and thymine derivatives in several solvents. Correlation between band frequencies and hydrogen-bonding states of the nucleic acid bases, J. Mol. Struct. 242 (1991) 87–98 https://doi.org/10.1016/0022-2860(91)87129-6
[55] I. Mukerji, A.P. Williams, UV resonance Raman and circular dichroism studies of a DNA duplex containing an A(3)T(3) tract: evidence for a premelting transition and three-centered H-bonds, Biochemistry 41 (2002) 69–77 https://doi.org/10.1021/bi010918i
[56] M. Tsuboi, M. Komatsu, J. Hoshi, E. Kawashima, T. Sekine, Y. Ishido, M.P. Russell, J.M. Benevides, G.J. Thomas, Raman and infrared spectra of (2'S)-[2'-2H]Thymidine: vibrational coupling between deoxyribosyl and thymine moieties and structural implications, J. Am. Chem. Soc. 119 (1997) 2025–2032 https://doi.org/10.1021/ja962760
[57] A. Jirasek, H.G. Schulze, C.H. Hughesman, A.L. Creagh, C.A. Haynes, M.W. Blades, R.F.B. Turner, Discrimination between UV radiation-induced and thermally induced spectral changes in AT-paired DNA oligomers using UV resonance Raman spectroscopy, J. Raman Spectrosc. 37 (12) (2006) 1368– 1380 https://doi.org/10.1002/jrs.1552
[58] B. Tomlinson, W.L. Peticolas, Conformational dependence of Raman scattering intensities in Polyadenylic acid, J. Chem. Phys. 52 (1970) 2154 https://doi.org/10.1063/1.1673270
[59] B. Rossi, M. Tortora, S. Catalini, J. Vigna, I. Mancini, A. Gessini, C. Masciovecchio, A. Mele, Insight into the thermal stability of DNA in hydrated ionic liquids from multi-wavelength UV resonance Raman experiments, Phys. Chem. Chem. Phys. 23 (2021) 5980-15988 https://doi.org/10.1039/D1CP01970H
[60] S.C. Erfurth, W.L. Peticolas, Melting and premelting phenomenon in DNA by laser Raman scattering, Biopolymers 14 (2) (1975) 247–264 https://doi.org/10.1002/bip.1975.360140202
[61] L. Movileanu, J.M. Benevides, G.J. Thomas Jr, Determination of base and backbone contributions to the thermodynamics of premelting and melting transitions in B DNA, Nucleic Acids Res. 30 (17) (2002) 3767–3777 https://doi.org/10.1093/nar/gkf471
[62] L. Rimai, V.M. Maher, D. Gill, I. Salmeen, J.J. McCormick, The temperature dependence of Raman intensities of DNA. Evidence for premelting changes and correlations with ultraviolet spectra, Biochim. Biophys. Acta. 361 (1974) 155–165 https://doi.org/10.1016/0005-2787(74)90343-8

[63] A. Chandran, D. Ghoshdastidar, S. Senapati, Groove binding mechanism of ionic liquids: A key factor in long-term stability of DNA in hydrated ionic liquids, J. Am. Chem. Soc. 134 (50) (2012) 20330–20339, https://doi.org/10.1021/ja304519d
[64] M.A. Young, B. Jayaram, D.L. Beveridge, Intrusion of counterions into the spine of hydration in the minor groove of B-DNA: fractional occupancy of electronegative pockets, J. Am. Chem. Soc. 119 (1) (1997) 59–69 https://doi.org/10.1021/ja960459m
[65] M.E. Di Pietro, M. Tortora, C. Bottari, G. Colombo Dugoni, R. Pivato, B. Rossi, M. Paolantoni, A. Mele, In Competition for Water: Hydrated Choline Chloride:Urea vs Choline Acetate:Urea Deep Eutectic Solvents, ACS Sustain. Chem. Eng. 9 (36) (2021) 12262–12273 https://doi.org/10.1021/acssuschemeng.1c03811
[66] A. Triolo, M. E. Di Pietro, A. Mele, F. Lo Celso, M. Brehm, V. Di Lisio, A. Martinelli, P. Chater, O. Russina, Liquid structure and dynamics in the choline acetate:urea 1:2 deep eutectic solvent. J. Chem. Phys. 154 (2021) 244501 https://doi.org/10.1063/5.0054048
[67] P. Del Vecchio, D. Esposito, L. Ricchi, G. Barone, The effects of polyols on the thermal stability of calf thymus DNA, Int. J. Biol. Macromol. 24 (1999) 361–369 https://doi.org/10.1016/S0141-8130(99)00058-6
[68] A.V. Lukashin, A.V. Vologodskii, M.D. Frank-Kamenetskii, Y.L. Lyubchenko, Fluctuational opening of the double Helix as revealed by theoretical and experimental study of DNA interaction with formaldehyde, J. Mol. Biol. 108 (1976) 665–682 https://doi.org/10.1016/s0022-2836(76)80111-8
[69] A.M.J.J. Bonvin, M. Sunnerhagen, G.O.Wilfred, F. van Gunsteren. Water molecules in DNA recognition II: amolecular dynamics viewof the structure and hydration of the trp operator, J. Mol. Biol. 282 (1998) 859–873 https://doi.org/10.1006/jmbi.1998.2034

Highlights

- the effect of choline-based DES on stability of double-stranded DNA is investigated
- DES improve the thermal stabilization of double-stranded canonical DNA structure
- hydration shell of AT pairs is strongly perturbed in the presence of DES
- preferential interaction between HB sites of guanine residues and DES is detected
- minor groove of DNA is significantly selective for the choline part of DES

Declaration of competing interest

The authors declare that they have no known competing financial interests or personal relationships that could have appeared to influence the work reported in this paper.

Author Statement

B.R. Conceptualization; B.R., M.T.,F.F.,J.V.,I.M. Data curation; B.R.,F.F. Formal analysis; C.M. Funding acquisition; B.R., J.V., M.T., A.G. Investigation; Methodology; Project administration; Resources; A.G. Software; B.R., B.M., A.M. Supervision; A.M., I.M.,J.V, B.M. Validation; Visualization; B.R., A.M.,B.B, J.V., I.M. Roles/Writing – original draft; B.R., A.M.,B.B, J.V., I.M. Writing – review & editing